J Am Oil Chem Soc (2009) 86:1215–1225
DOI 10.1007/s11746-009-1452-x

ORIGINAL PAPER

Characterization of Olive-Leaf Phenolics by ESI-MS and Evaluation of their Antioxidant Capacities by the CAT Assay

Mickaël Laguerre · Luis Javier López Giraldo · Georges Piombo · Maria Cruz Figueroa-Espinoza · Michel Pina · Mohamed Benaissa · Aurélia Combe · Anne Rossignol Castera · Jérôme Lecomte · Pierre Villeneuve

Received: 20 February 2009 / Revised: 27 July 2009 / Accepted: 28 July 2009 / Published online: 14 August 2009

Abstract Olive leaves are a very abundant vegetable material containing various phenolic compounds, such as secoiridoids and flavonoids, that are expected to exert strong antioxidant capacity. However, little is known about the variation of olive-leaf phenolic composition during maturation and its influence on antioxidant capacity. To answer this question, young and mature *Olea Europaea* L. leaves were submitted to successive extraction with dichloromethane, ethyl acetate, and methanol, then characterized by ESI-MS. It appeared that mature olive-leaf extracts contained higher levels of verbascoside isomers and glucosylated forms of luteolin, while young ones presented higher contents of oleuropein, ligstroside, and flavonoid aglycones. Moreover, antioxidant capacity evaluation using our newly developed conjugated autoxidizable triene assay showed that, in a lipid-based emulsified system, this phenolic composition variation leads to a change in the ability of extracts to counteract lipid oxidation. Mature olive-leaf extracts exhibit higher antioxidant capacity than young olive-leaf extracts. This result enables us to hypothesize that two main bioconversion scenarios may occur during maturation of olive leaves, which could explain changes observed in antioxidant capacity: (1) a bioconversion of oleuropein and ligstroside into verbascoside isomers and oleuroside, and (2) a bioconversion of flavonoid aglycones into glucosylated forms of luteolin. Finally, this study leads to a better understanding of the relationship between phenolic profile and antioxidant capacity of olive leaves.

Keywords Olive leaves · Antioxidant · Phenolics · Oleuropein · Verbascoside · Quercetin · Bioconversion · CAT assay

M. Laguerre · L. J. López Giraldo · G. Piombo · M. C. Figueroa-Espinoza · M. Pina · J. Lecomte · P. Villeneuve (✉)
Cirad , Persyst, UMR IATE, 34398 Montpellier, France
e-mail: villeneuve@cirad.fr; pierre.villeneuve@cirad.fr

M. C. Figueroa-Espinoza
IRC, Montpellier SupAgro, 1101 av. Agropolis, BP 509834093 Montpellier, France

M. Benaissa
Faculté des Sciences, Université Hassan II-Ain Chock, Casablanca, Morocco

A. Combe · A. Rossignol Castera
L'Olivie SAS, Mas de Fourque, 34980 Combaillaux, France

Introduction

For many centuries, olive leaves have been associated with health and preservation. Ancient Egyptians used them to mummify their pharaohs [1]. Later, olive leaves were used as a folk remedy to fight various diseases. The first formal report of medicinal use was made in 1854, when olive-leaf extract was reported to be effective in treating fever and malaria [2]. In recent times, several studies have shown that olive-leaf extracts exhibit a large spectrum of in vitro and in vivo properties, including antioxidant capacity [3–7], antifungal activity [8], antibacterial activity [9], anti-HIV property [10], vasodilator effect [11], and hypoglycemic effect [12].

In the cultivation of the olive tree, the pruning step generates a considerable volume of biomass, which constitutes the main source of olive leaves. Considering that it is a very abundant vegetable material, it is justified that important scientific and technical efforts are made to determine the value of this agricultural residue. Among the

different possible applications, the use of olive-leaf extract to counteract oxidative damages in food, and even in human health, seems to be very promising.

With regard to this matter, olive-leaf extracts present several potential antioxidant molecules, essentially belonging to the phenolic family. In the second part of the last century, a phenolic compound, characterized as a secoiridoid and called oleuropein, found in *Olea europaea* tree and fruit oil was isolated from olive leaves [13]. This bitter compound, the most-reported constituent of the secoiridoid family in the olive tissues, is a hydroxytyrosol ester with β-glucosylated elenolic acid (Fig. 1). Other secoiridoids derived from tyrosol backbone, such as ligstroside, oleuroside, and verbascoside, were also identified in olive-leaf extracts (Fig. 1). Besides secoiridoids, various flavonoids are also present in olive leaves, either in an aglycone form (quercetin, apigenin, luteolin, diosmetin) or in a glycosylated one (quercetin-7-*O*-rutinoside, luteolin-7-*O*-rutinoside, luteolin-7-*O*-glucoside, luteolin-5-*O*-glucoside). This phenolic profile can drastically change according to the variety, the geographical location, and the agroecological conditions, especially seasons. Heimler et al. [14] showed that luteolin and luteolin-7-glucoside reached a maximum level in spring, while levels of luteolin-4-glucoside and chlorogenic acid showed a maximum in early winter. Some other compounds such as quercitrin and apigenin do not significantly vary according to the season. Recently, Fabbri et al. [15] observed that cultivar and collection time caused large variations in the total amount of the different components. The maximum content of polyphenols and secoiridoids was found in December (winter).

Besides these variations, to the best of our knowledge, little is known about the chemical variations occurring during maturation of olive leaves in relation to their antioxidant capacities. One of the main difficulties is the assessment of the antioxidant capacity of these leaf extracts since a multitude of tests are available, but none of them are universal [16]. Recently, we developed a microplate reader method called conjugated autoxidizable triene (CAT) assay [17]. This in vitro test is based on spectral properties of TAGs naturally present in the commercially available *Aleurites fordii* seed oil (tung oil). These TAGs contain around 85% eleostearic acid, an octadecatrienoic acid with three conjugated double bonds, exhibiting a strong UV absorption at 273 nm. In dispersion in water and under oxidizing conditions, the degradation of TAGs' conjugated trienes is accompanied by a bleaching at 273 nm. Addition of antioxidant molecules or extracts rich in antioxidants results in a delay in oxidation and enables quantification of the antioxidant capacity in comparison with a reference standard (Trolox).

The purpose of this study was to identify the main phenolic compounds present in three different extracts of young and mature olive leaves by the use of electrospray ionization mass spectrometry. A second objective was to investigate how differences in this chemical profile can impact the antioxidant capacity of olive-leaf extracts using the CAT assay.

Materials and Methods

Chemicals

Tung oil from *A. fordii* seeds (tung oil, averaged MW = 872 g/mol) was purchased from Aldrich Chemical (Ref. 440337). Phosphate buffer solution pH 7.2 (PBS)

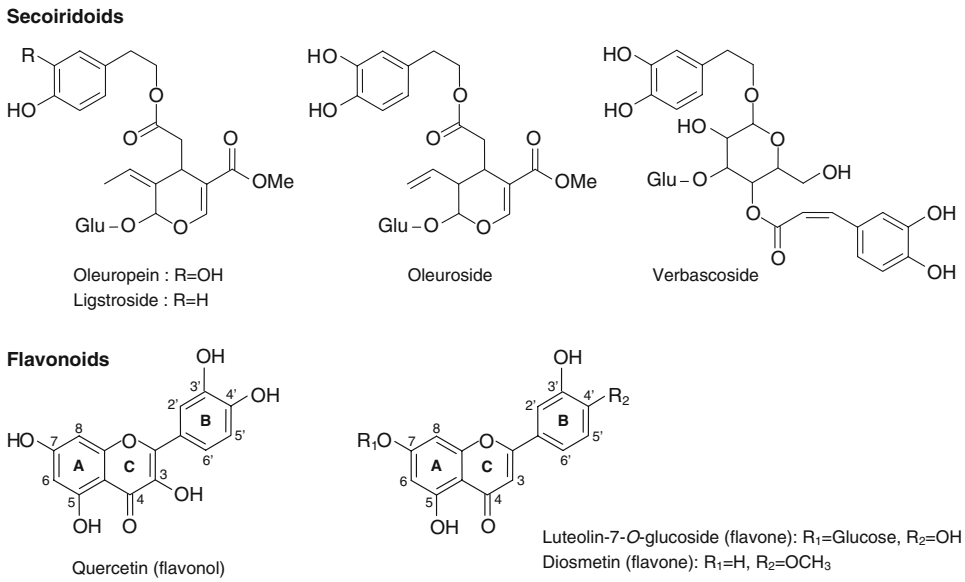

Fig. 1 Flavonoids and secoiridoids present in olive leaves

and polyoxyethylene(23)laurylether (Brij 35, estimated MW = 1,198 g/mol) were purchased from Sigma (Saint Quentin, France). Oleuropein and luteolin-7-*O*-glucoside were purchased from Extrasynthèse (Genay, France). All solvents used were HPLC or analytical grade and were purchased from Sigma (Saint Quentin, France). Trolox was purchased from Acros Organic (Geel, Belgium) and 2,2′-azobis(2-amidinopropane) dihydrochloride (AAPH) from Wako Chemical (Neuss, Germany).

Preparation of Olive-Leaf Extracts

In order to avoid possible bias, all Picholine olive leaves (*Olea europea*) were collected during the same day on 10 trees in June 2007 at Domaine de l'Olivie (Combaillaud, south of France). Young (~50 g) and mature (~50 g) olive leaves were 1 and 3 years old, respectively. They were frozen in liquid nitrogen, freeze-dried for 24 h in a cryodessicator at 10^{-3} atm (Alpha 1-4, Fisher Bioblock Scientific, Marseille, France), ground, and then sieved at 1 mm. To remove neutral lipids, a solid–liquid extraction with hexane (five cycles of 7 min at 60 °C, 100 bars) was performed on the resulting samples (powder) using an ASE 200 automatic extractor (accelerated solvent extraction, Dionex SA, Voisin Le Bretonneux, France). The insoluble fraction was then submitted to successive extractions of 7 min each at 100 bars in the same apparatus as follows: dichloromethane (five cycles at 40 °C), ethyl acetate (five cycles at 80 °C), and methanol (five cycles at 80 °C) (Fig. 2). For each organic phase, the solvent was evaporated under vacuum using a rotary evaporator, and the residue was submitted to a nitrogen stream until constant weight. Finally, the obtained extracts were stored at 4 °C in brown flasks (UV filter) until use.

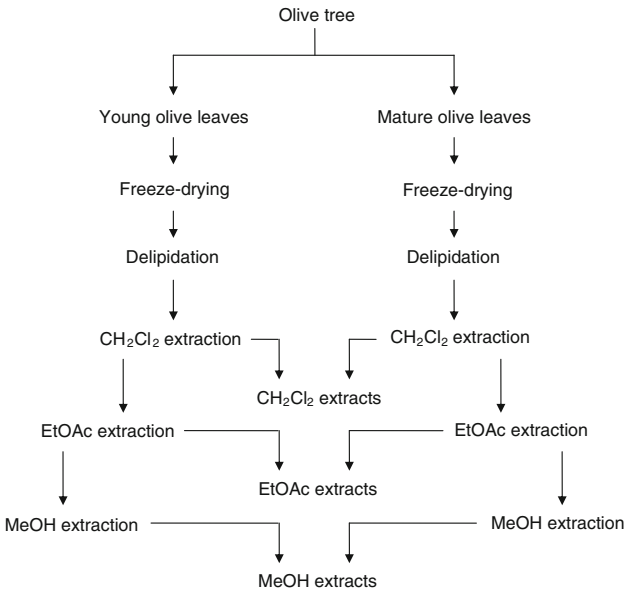

Fig. 2 Successive extraction flow chart

HPLC/MS-ESI Characterization

Olive-leaf extracts were dissolved in methanol at 4 mg/mL. Then, 20 μL of these solutions was filtered (0.45 μm) and injected in an HPLC instrument (Thermo Fisher, San Jose, CA, USA) coupled with a mass spectrometer (Thermo Fisher).

The LC system used was composed of an injection loop, an automatic sampler, and a photodiode detector array (PDA). Compounds were separated on an ACE C-18 column (5 μm, 250 × 4.6 mm, Houilles, France) at a flow rate of 0.3 mL/min, using as solvent A, a mixture of water/formic acid (99.9:0.1 v/v) and as solvent B, a mixture of acetonitrile/water/formic acid (80:19.9:0.1 v/v/v). The elution was performed in a linear gradient from 97 to 65% A over 50 min, from 65 to 50% A over 5 min, from 50 to 20% A over 5 min, from 20 to 0% A over 10 min, and finally returning to the initial conditions for 10 min.

The MS system (Thermo Finnigan, San Jose, CA, USA) was composed of a quadrupole ion trap, an external ionization source operating at atmospheric pressure, and an integrated injector system. The data acquisition in negative-ion electrospray ionization (ESI)-MS was achieved in full scan mode (MS mode), but also after fragmentation of parent ion (MS^2 mode). Analysis conditions were fixed as follows: ionization voltage, 4.54 kV; capillary temperature, 250 °C; nitrogen flow, 20 (arbitrary units); collision energy in MS^2 mode, 30–35%.

Preparation of Tocopherol-Free Tung Oil Samples

The polar compounds of tung oil (including β-tocopherol) were removed by passing 25 mL of a 200 mg/mL tung oil solution in hexane, followed by 25 mL of pure hexane through an alumina column prepared as follows: 25 g of alumina in hexane was introduced into a glass column, and the excess hexane was eliminated until it rose to the alumina surface. After complete removal of tocopherols, hexane was evaporated under vacuum at 35 °C using a rotatory evaporator equipped with a vacuum pump (Laborport, KNF Neuberger, Freiburg, Germany). It is worth noting that all experiments must be carried out sheltered from light as much as possible. Finally, the stripped tung oil was aliquoted into brown glass tubes, then flushed with nitrogen, and stored at −18 °C until use. The use of disposable stripped tung oil aliquots (i.e., 15 aliquots for 15 microplates) avoids the necessity for successive withdrawals from one aliquot and minimizes any possible oxidation.

Conjugated Autoxidizable Triene Assay Protocol

(1) Antioxidant capacity of olive-leaf extract was measured using the CAT procedure previously described [17] with some slight modifications. Briefly, antioxidant solutions were prepared as follows: a methanol solution of olive-leaf extract or Trolox (reference) was prepared at the desired concentration. It is worth mentioning that the olive-leaf extract solutions must be filtered (0.45 μm) to remove impurities which can interfere in the CAT value measurement. Then, various volumes of this solution (25, 50, 75, and 100 μL) were added to 24.9 mL of phosphate buffer solution (PBS), pH 7.2, and then filled to 25.0 mL with pure methanol (75, 50, 25, and 0 μL, respectively). In this way, all buffered solutions of olive-leaf extract contain the same methanol volume (100 μL), which minimizes any possible bias among samples. This new CAT procedure enables the analysis of a larger panel of molecules from hydrophilic to lipophilic ones. Moreover, phenolic compounds in methanol solutions are far more stable than in PBS, thus allowing storage at −20 °C for several days, which is not possible with PBS. All buffered solutions of olive-leaf extract or Trolox were prepared in this way daily. Samples of these solutions (50 μL/well) were transferred using a multichannel micropipet into UV-Star 96-well microplate (Greiner, Frickenhausen, Germany) (absorbance at 273 nm = 0.03). The microplate was then prewarmed and stirred in a thermostated shaker (PHMT Grant Instruments, Shepreth, England) at 37 °C for 5 min at 1,200 rpm.

(2) Twenty-five milliliters of a buffered solution (pH 7.2) containing 34 μM Brij 35 (neutral emulsifier, estimated MW = 1,198 g/mol) was added to 5 mg stripped tung oil in a brown glass flask. For the next step, it was crucial to premix this mixture by stirring it for 10 s using a Vortex apparatus, before its homogenization in an Ultra Turrax homogenizer (Janke & Kunkel, Staufen, Germany) at approximately 2,400 rpm for 90 s. Each well was then filled with 100 μL of this tung oil-in-PBS emulsion. To improve repeatability, the microplate was then immediately pre-warmed and shaken, sheltered from light, in a thermostated shaker (PHMT Grant Instruments) at 37 °C for 1 min at 1,200 rpm.

(3) Fifty microliters of a freshly prepared AAPH solution in PBS (4 mM) was added with a multichannel micropipet. In the end, each well contained 200 μL of the final mixture consisting of 115 μM stripped tung oil, 17 μM Brij 35, 1 mM AAPH, and various concentrations of Trolox (from 0 to 2 μM) and extracts (from 0.8 to 3.2 mg/L for both ethyl acetate and methanol extracts and from 2.4 to 9.6 mg/L for dichloromethane extract) in PBS. The progress of reactions was immediately monitored by recording the decrease in absorbance at 273 nm. Measurements were performed each minute for 5 h at 37 ± 0.1 °C, with 5 s of stirring before each measure, using a Saffire 2 microplate reader (Tecan, Gröedig, Austria) equipped with Magellan software. Each experiment was performed in triplicate (three wells), and results were expressed as the mean of CAT value (see below) ± SD.

To normalize data, the raw absorbance signal was transformed to relative absorbance according to the following equation:

$$\text{Relative absorbance} = A_t/A_0 \quad (1)$$

where A_t and A_0 are absorbances read at times t and 0 min, respectively. It is worth mentioning that if the measurement is not rapid enough after AAPH addition, the A_0 for the blank (without antioxidant) may be far lower than that of the sample containing antioxidant. In this case, to normalize A_0, the experimental A_0 for the blank could be artificially replaced by the A_0 of samples in Eq. 1.

The area under the curve (AUC) corresponding to relative absorbance decay was calculated as:

$$\text{AUC} = 1 + A_1/A_0 + A_2/A_0 + \cdots + A_{299}/A_0 + A_{300}/A_0 \quad (2)$$

The net protection area provided by an olive-leaf extract was then calculated using the difference between the AUC in the presence of an olive-leaf extract ($AUC_{Extract}$) and the AUC of the blank (AUC_{Blank}), the latter consisting of the same mixture without olive-leaf extract.

Trolox was used as a calibrator for antioxidant capacity measurements. Thus, the antioxidant capacity (or the CAT value) of an olive-leaf extract relative to Trolox is given as:

$$\text{CAT value} = [(AUC_{Extract} - AUC_{Blank})/(AUC_{Trolox} - AUC_{Blank})] \times [\mu\text{mole of Trolox/g of dried extract}] \quad (3)$$

where $(AUC_{Extract} - AUC_{Blank})$ and $(AUC_{Trolox} - AUC_{Blank})$ are the net protection areas in the presence of an olive-leaf extract and Trolox, respectively. It is crucial that Trolox was used as internal calibrator (i.e., analyzed on the same microplate). Finally, the CAT value was expressed as micromoles of Trolox equivalent (TE) per gram of dried extract.

Results and Discussion

Characterization of Olive-Leaf Extracts by HPLC/MS-ESI

HPLC/MS-ESI characterization in negative mode was achieved on dichloromethane (Fig. 3), ethyl acetate

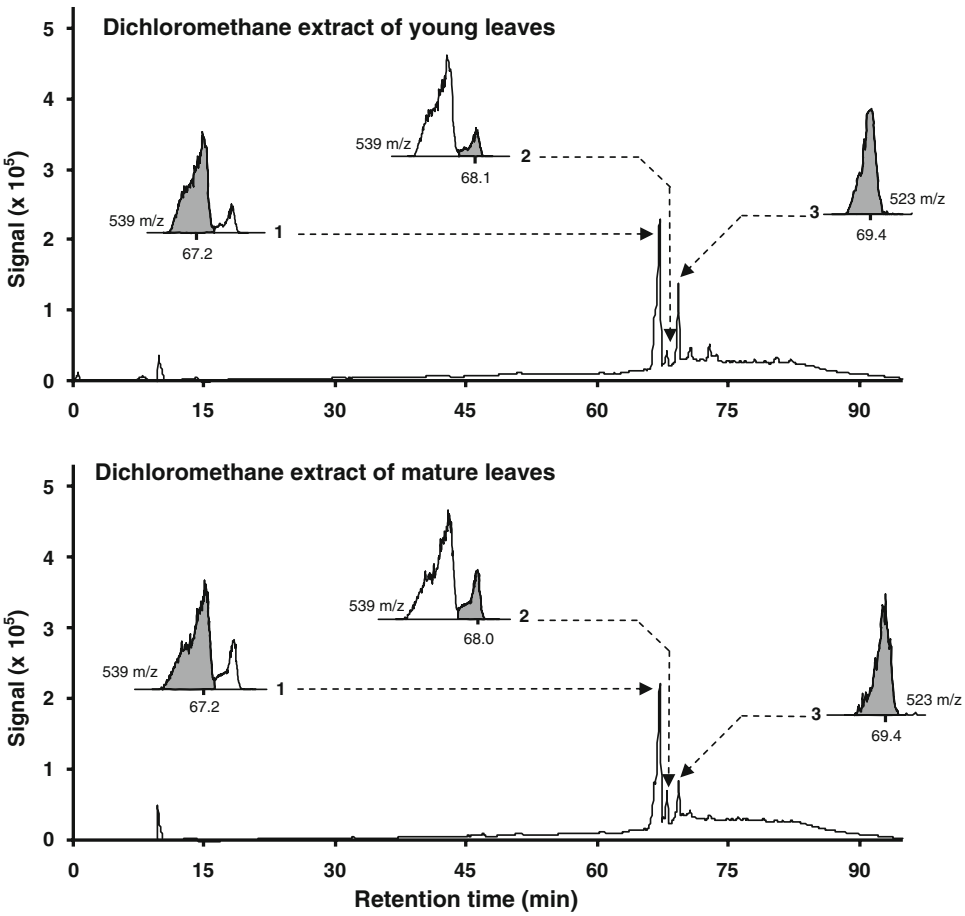

Fig. 3 Reconstructed PDA chromatograms obtained from dichloromethane extracts of young (*upper graph*) and mature (*lower graph*) olive leaves. The PDA detection was performed between 200 and 700 nm at intervals of 1 nm. *Gray peaks* in *insets* correspond to $[M–H]^-$ ion (of each compound) extracted from full MS scan chromatograms. All dry extracts were solubilized in methanol at 4 mg/mL, filtered (0.45 μm), and 20 μL was injected in HPLC. *Peak numbers* correspond to compounds given in Table 1

(Fig. 4), and methanol (Fig. 5) extracts of both young and mature olive leaves. In addition to these chromatograms, Table 1 lists each of the identified phenolic compounds in elution order. Briefly, identification of phenolic compounds was based on the search for pseudomolecular $[M–H]^-$ ions [obtained in full scan (or MS) mode], together with the interpretation of its collision-induced dissociation fragments (obtained in MS^2 mode). When authentic standards were available, identification was carried out by comparing retention times and mass spectra (MS) with these standards.

First, the HPLC/MS-ESI analysis of dichloromethane extracts of both young and mature olive leaves (Fig. 3; Table 1) showed a simple chemical profile. The MS and MS^2 of the two first peaks arising at ~67.2 (A1) min and ~68.1 (A2) min both display precursor ion at m/z 539 and a precursor-derived ion at m/z 377. Precursor ion (m/z 539) corresponds to the pseudomolecular $[M–H]^-$ ion of both oleuropein and its isomer oleuroside (Fig. 1), whose molecular masses are 540. The m/z 377 ion derived from the fragmentation of the pseudomolecular $[M–H]^-$ ion corresponds to the oleuropein aglycone or oleuroside aglycone, resulting from the loss of a glucose moiety. Further experiment showed that A1 was superimposable with that of standard oleuropein, allowing clear attribution of oleuropein to this peak, and oleuroside to peak A2. The third peak arising at 69.4 (A3) min is a deoxy analogue of oleuropein, named ligstroside (Fig. 1). Its presence seems to be supported by the presence of a pair of ions at m/z 523/361. Indeed, these ions are identical to that of the oleuropein (m/z 539/377) with the difference that both ions are downshifted by 16, which corresponds to a deoxy oleuropein.

Concerning the ethyl acetate extracts, 10 compounds were identified in both young and mature olive leaves (Fig. 4; Table 1). First, peaks B1 and B2 detected at ~55.8 and ~56.7 min (only present in appreciable levels in extract of mature olive leaves) correspond to verbascoside isomers. The m/z 623 ion corresponded to the pseudomolecular $[M–H]^-$ ion of verbascoside, which is a heterosidic ester of caffeic acid and hydroxytyrosol (Fig. 1). Then, the MS and MS^2 of the peaks arising at ~57.8 (B3) min and ~64.2 (B4) min both display a precursor ion at m/z 447, corresponding to the pseudomolecular $[M–H]^-$ ion of luteolin-glucoside, and the precursor-derived m/z 285 ion, corresponding to the luteolin aglycone as a result of the loss of a glucose moiety. Moreover, B3 is superimposable with that of standard

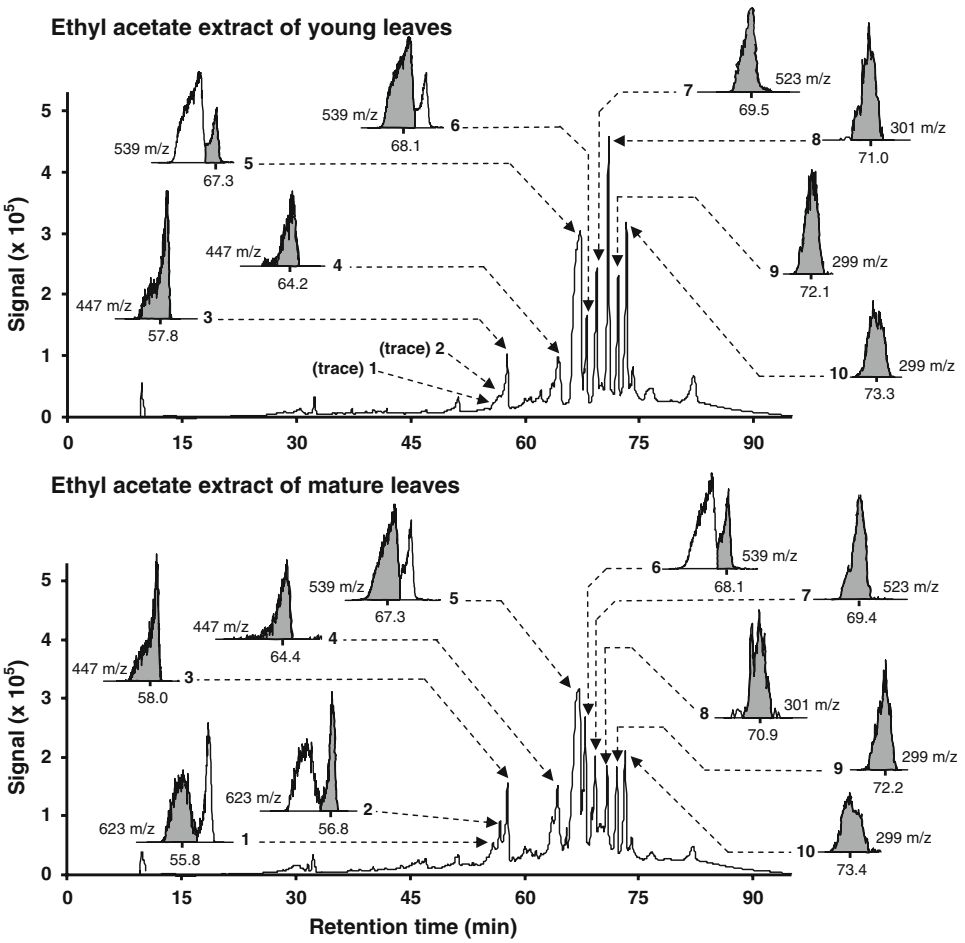

Fig. 4 Reconstructed PDA chromatograms obtained from ethyl acetate extracts of young (*upper graph*) and mature (*lower graph*) olive leaves. The PDA detection was performed between 200 and 700 nm at intervals of 1 nm. *Gray peaks* in *insets* correspond to $[M–H]^-$ ion (of each compound) extracted from full MS scan chromatograms. All dry extracts were solubilized in methanol at 4 mg/mL, filtered (0.45 µm), and 20 µL was injected in HPLC. *Peak numbers* correspond to compounds given in Table 1

luteolin-7-*O*-glucoside. The three peaks arising at ~67.3 (B5) min, ~68.1 (B6) min, and ~69.5 (B7) min, correspond to oleuropein, oleuroside, and ligstroside since they exhibit identical MS, MS^2, and retention times as A1, A2, and A3 in dichloromethane extracts, respectively. The peak B8 detected at ~71 min corresponds to the quercetin aglycone because of the MS display at m/z 301, corresponding to the pseudomolecular ion $[M–H]^-$ ion of quercetin aglycone. The two last peaks detected at ~72.1 (B9) min and ~73.3 (B10) min were characterized as isomers of diosmetin aglycone, based on the MS m/z 299 ion, corresponding to the pseudomolecular $[M–H]^-$ ion of diosmetin aglycone.

Finally, the methanolic extracts of young and mature olive leaves (Fig. 5; Table 1) exhibit the same compounds already observed in ethyl acetate extracts. Thus, verbascoside isomers (C1 and C2 only present at appreciable levels in methanolic extract of mature leaves) at ~55.6 and ~56.7 min, luteolin-7-*O*-glucoside (C3) at ~57.8 min, an unidentified isomer of luteolin-glucoside (C4) at ~64.4 min, oleuropein (C5) at ~67.1 min, oleuroside (C6) at ~68 min, ligstroside (C7) at ~69.5 min, quercetin (C8) at ~70.8 min, and two isomers of diosmetin aglycone (C9, 10) at ~72.2 and ~73.2 min were identified in methanolic extracts.

Study of the Evolution of the Phenolic Profile

Peak resolution of PDA-reconstructed chromatograms, especially from methanol extracts, renders peak area calculations difficult. To obtain a better resolution, on chromatograms reconstructed from negative full scan MS, a systematic study of the previously identified phenolics was carried out by extracting the corresponding $[M–H]^-$ ion (insets of Figs. 3, 4, 5). From these MS profiles, peak areas could be satisfactorily calculated. Obviously, it is worth mentioning that this process does not enable us to compare different compounds in quantitative terms because both response factors and ionization conditions are not identical from one compound to another. However, it allows studying the evolution of the relative proportion of a given compound in different chromatograms. Thus, the relative proportion of a given compound analyzed in different extracts is expressed as a percentage of the maximum level of this same compound encountered in the extracts. For example, the level of oleuropein in ethyl acetate extract of

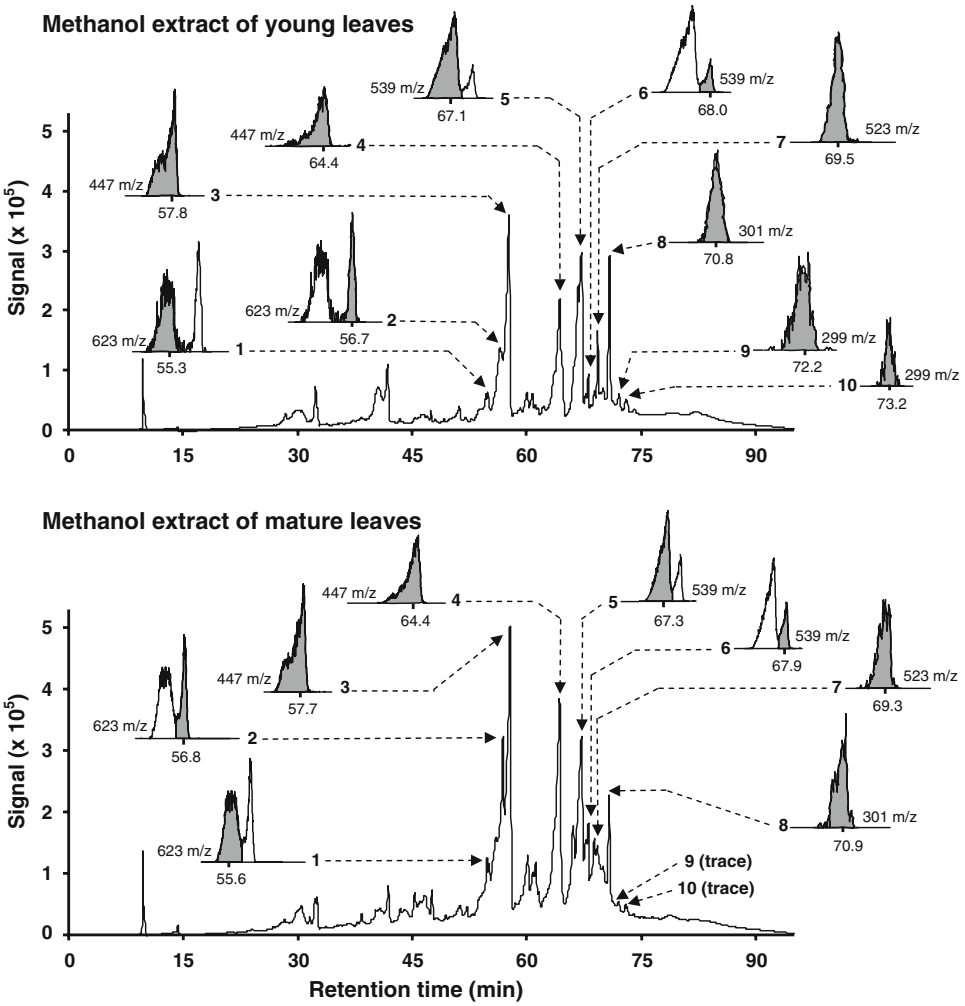

Fig. 5 Reconstructed PDA chromatograms obtained from methanolic extracts of young (*upper graph*) and mature (*lower graph*) olive leaves. The PDA detection was performed between 200 and 700 nm at intervals of 1 nm. *Gray peaks* in *insets* correspond to $[M–H]^-$ ion (of each compound) extracted from full MS scan chromatograms. All dry extracts were solubilized in methanol at 4 mg/mL, filtered (0.45 μm), and 20 μL was injected in HPLC. *Peak numbers* correspond to compounds given in Table 1

young leaf was considered as the maximum level (100%), and the relative proportion of oleuropein in other extracts has been established in comparison to the 100% values. This semiquantitative calculation applied to each compound leads to Fig. 6 for secoiridoids and Fig. 7 for flavonoids, allowing the study of the relative proportion of phenolics according to the maturation degree of olive leaves. Because the two isomers of verbascoside vary in the same way, their peak areas were summed to give Fig. 6a. The same calculation was carried out with the two glucosylated forms of luteolin (Fig. 7a) and the two diosmetin isomers (Fig. 7c).

Regardless of the solvent extraction used, results have shown that the maturation of olive leaves leads to a decrease in oleuropein (except in CH_2Cl_2 extract), ligstroside, quercetin, and diosmetin aglycone isomers, with a simultaneous increase in levels of verbascoside, glucosylated forms of luteolin, and finally oleuroside (Figs. 6, 7). To the best of our knowledge, there is a gap in the available data dealing with the effect of maturation of olive leaves on their chemical profile. However, a parallel can be found in other olive-derived products such as olive fruit. Interestingly, Amiot et al. [18] have established a similar inverse relationship between oleuropein content in olive fruit and verbascoside, and have showed that the latter cannot be detected in very young olive fruit. Amiot et al. [18] have hypothesized that there is a metabolic relationship between oleuropein and verbascoside because they both share the same hydroxytyrosol moiety (Fig. 1). So, the same bioconversion of oleuropein in verbascoside could also occur during maturation of olive leaves (Fig. 6). Moreover, as for verbascoside isomers, oleuroside level increases concomitantly with the decrease in both oleuropein and ligstroside. Because these four secoiridoids share a very similar molecular structure, it is also likely that bioconversion of oleuropein and/or ligstroside to oleuroside and/or verbascoside occurs during maturation.

To verify that oleuroside and verbascoside were not metabolic products of other compounds containing such a molecular structure (secoiridoid-hydrolyzed derivatives), a systematic study of tyrosol and hydroxytyrosol was undertaken by extracting the corresponding $[M–H]^-$ ion

Table 1 Phenolic compounds detected in dichloromethane, ethyl acetate, and methanol extracts of young and mature olive leaf in elution order, and corresponding ESI/MS data in negative mode

Compound	Peak	MW	MS $[M-H]^-$ (m/z)	MS^2 (m/z)	Young leaves RT (min)	Mature leaves RT (min)
Dichloromethane extract						
Oleuropein	A1	540	539	377	67.2	67.2
Oleuroside	A2	540	539	377	68.1	68.0
Ligstroside	A3	524	523	361	69.4	69.4
Ethyl acetate extract						
Verbascoside (isomer 1)	B1	624	623	–	55.8 (trace)	55.8
Verbascoside (isomer 2)	B2	624	623	–	56.7 (trace)	56.8
Luteolin-7-*O*-glucoside	B3	448	447	285	57.8	58.0
Luteolin-glucoside isomer	B4	448	447	285	64.2	64.4
Oleuropein	B5	540	539	377	67.3	67.3
Oleuroside	B6	540	539	377	68.1	68.1
Ligstroside	B7	524	523	361	69.5	69.4
Quercetin	B8	302	301	–	71.0	70.9
Diosmetin aglycone (isomer 1)	B9	300	299	–	72.1	72.2
Diosmetin aglycone (isomer 2)	B10	300	299	–	73.3	73.4
Methanol extract						
Verbascoside (isomer 1)	C1	624	623	–	55.3	55.6
Verbascoside (isomer 2)	C2	624	623	–	56.7	56.8
Luteolin-7-*O*-glucoside	C3	448	447	285	57.8	57.7
Luteolin-glucoside isomer	C4	448	447	285	64.4	64.4
Oleuropein	C5	540	539	377	67.1	67.3
Oleuroside	C6	540	539	371	68.0	67.9
Ligstroside	C7	524	523	361	69.5	69.3
Quercetin	C8	302	301	–	70.8	70.9
Diosmetin aglycone (isomer 1)	C9	300	299	–	72.2	72.1 (trace)
Diosmetin aglycone (isomer 2)	C10	300	299	–	73.2	73.2 (trace)

Peak number corresponds to compounds given in Figs. 3, 4, and 5

MW Molecular weight, *MS* $[M–H]^-$ pseudomolecular ion obtained by electrospray ionization mass spectrometry in full scan (MS mode), MS^2 collision-induced dissociation fragments (obtained in MS^2 mode) of pseudomolecular ion, *RT* retention time

from reconstructed chromatograms, but no significant signal was observed. The apparent absence of these secoiridoid hydrolysis-derived products is not surprising, especially for hydroxytyrosol, which is known to be rarely found in the free form in nature [19], but rather in a glycosylated one. Furthermore, this result reinforces the hypothesis that oleuropein and ligstroside are the only molecules possessing hydroxytyrosol or tyrosol moiety to donate to verbascoside isomers and oleuroside.

In addition to secoiridoid evolution, we also observed that flavonoid aglycone (quercetin and diosmetin) reductions were accompanied by an increase in glucosylated forms of luteolin (Fig. 7). It is well known that the flavonoid aglycones, which have a variety of glycosylation sites, are converted into glycones by glycosyltransferase in the last step of flavonoid biosynthesis [20]. In agreement with our chromatographic data, flavonoids are likely stored in mature olive leaves as glycosylated forms, which is assumed to protect them from degradation, and, above all, to reduce their toxicity for the plant. So, in parallel with the bioconversion of secoiridoids, it is assumed that maturation of olive leaves is accompanied by a bioconversion of quercetin and diosmetin aglycone isomers in glucosylated forms of luteolin. It is also worth noting that glycosylation is not the only process involved in such a bioconversion. Indeed, addition of a 4′-hydroxyl group to the B ring of diosmetin (instead of the methoxyl group) and elimination of the 3-hydroxyl group in the C ring of quercetin constitute an important step in this putative bioconversion.

Antioxidant Capacity Evaluation by the CAT Assay

Antioxidant capacity of leaf extracts was evaluated by use of the newly developed CAT assay [17] using TAGs of

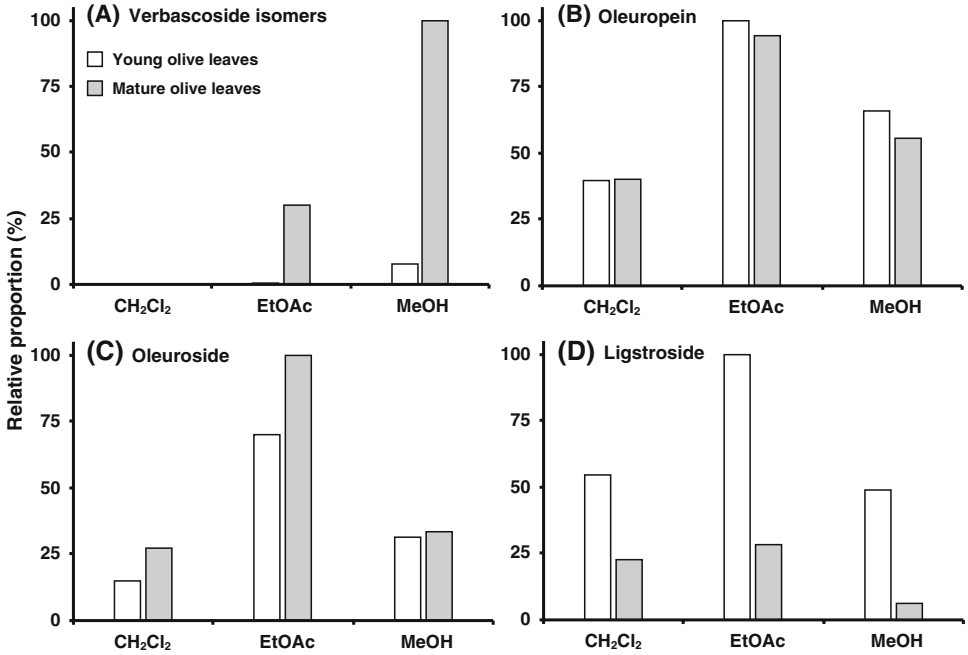

Fig. 6 Relative proportion of secoiridoids present in olive-leaf extracts. The relative proportion is calculated for a given compound as the percentage of the highest level of this compound encountered in one of the three extracts

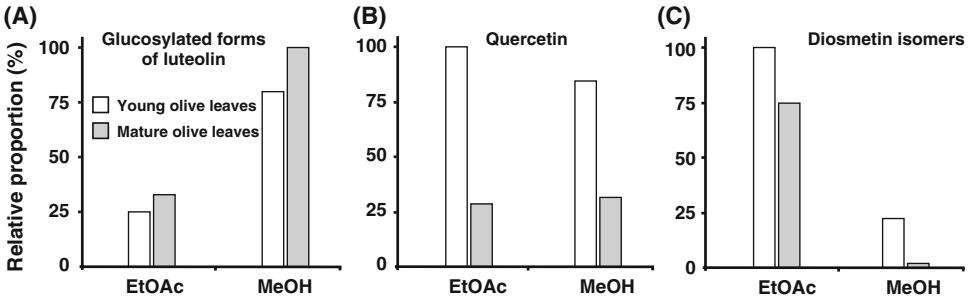

Fig. 7 Relative proportion of flavonoids present in olive-leaf extracts. The relative proportion is calculated for a given compound as the percentage of the highest level of this compound encountered in one of the three extracts

tung oil as an ultraviolet probe in an emulsified medium. Figure 8 illustrates the kinetics of bleaching in the absence or presence of olive-leaf extract (weight equivalents). These results clearly show that all extracts delay AAPH-induced oxidation of stripped tung oil, but none of them exhibits a significant lag phase, which allows, partially, for an estimation of their mechanism of action. Indeed, the absence of a lag phase is rather characteristic of the ability of leaf extracts to scavenge AAPH-derived peroxyl radicals, instead of a direct reduction of the lipoperoxyl radical derived from oil [17]. This kinetic behavior is likely to be linked to the relative hydrophilic nature of tested phenolic compounds, which are potentially far away from the oil/water interface where oxidation occurs.

In order to compare CAT values of olive-leaf extracts with antioxidant capacities established with other methodologies, Trolox was used as reference. Thus, this hydrophilic equivalent of α-tocopherol was analyzed on the same microplate (internal calibration) at four concentrations (0.4, 0.8, 1.2, and 1.6 μM, final concentration, data not shown). On the other hand, because leaf extracts (especially dichloromethane) contain very high levels of the strong chlorophyll chromophores, increasing concentration of olive-leaf extracts can lead to a slight spectral interference in the UV domain. Therefore, CAT value was calculated according to Eq. 3 only for leaf-extract concentrations given in Fig. 8 (i.e., 2.4 mg/L for dichloromethane and 0.8 mg/L for the two others).

The antioxidant capacity evaluation obtained by the CAT assay showed that, regardless of the solvent extraction used, mature-leaf extracts exert higher antioxidant capacity than young-leaf extracts (Fig. 9). CAT values of young olive-leaf dichloromethane extract were 146 ± 18 μmol Trolox equivalent (TE)/g of dried extract, while those of mature leaves were 211 ± 19 μmol TE/g of dried extract. In the same manner, for ethyl acetate and methanol extracts of young leaves, the CAT values were 1,178 ± 81 and 633 ± 83 μmol TE/g of dried extract, respectively, while those of mature leaves were 1,494 ± 6 and 873 ± 35 μmol TE/g of dried extract, respectively. These differences could be partially explained by the theorized bioconversion scenario. Indeed, verbascoside possesses two *o*-diphenolic

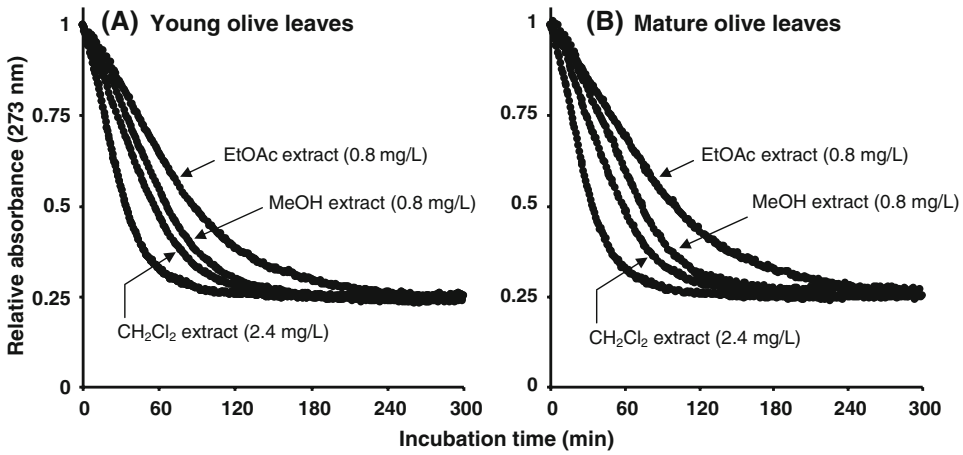

Fig. 8 Kinetics of relative absorbance bleaching in the absence and presence of (a) young and (b) mature olive-leaf extracts in stripped tung oil-in-water emulsion. The reaction mixture contained 115 μM tung oil, 17 μM Brij 35, 1 mM AAPH in PBS, pH 7.2, at 37 °C

(or catechol) moieties, oleuropein possesses one catechol, and ligstroside does not possess this structural feature. The catechol group is known to confer a high stability to the antioxidant radical because a strong H-bond is formed between the radical and the vicinal OH group after the homolytic breaking of the O–H bond. This H-bond establishment theoretically increases the radical stability and consequently decreases the O–H bond dissociation enthalpy of the corresponding phenolic hydroxyls [17, 21]. Therefore, the bioconversion of a noncatecholic (ligstroside) or monocatecholic (oleuropein) compound into a dicatecholic (verbascoside) one could explain the overall higher antioxidant capacity of mature-leaf extracts. Considering that the increase in the number of catechol structure(s) enhances the antioxidant capacity, the putative formation of oleuroside (one catechol) from ligstroside (zero catechol) is expected to lead to an increase in its ability to protect tung oil. In contrast, if oleuroside is an oleuropein-derived metabolite, no significant increase in the antioxidant properties of the corresponding extract is expected, since these two molecules possess the same catecholic moiety.

The bioconversion of diosmetin isomers (zero catechol) (Fig. 1), in glucosylated forms of luteolin (one catechol) could also explain the higher antioxidant capacity of mature leaf extracts. Nevertheless, it is more difficult to interpret the effect of the putative bioconversion of quercetin in glucosylated forms of luteolin on the antioxidant capacity. Indeed, it is generally assumed that quercetin containing (1) a 3,4-*o*-diphenol moiety on B ring, (2) a 4-keto-3-hydroxyl group on C ring conjugated to (3) a 2,3-double bond on the C ring is more able to scavenge free radicals than the corresponding flavones (i.e., luteolin) lacking the 3-hydroxyl moiety on the ring C [22]. Thus, a bioconversion of quercetin in luteolin, even in glucosylated form, is assumed to decrease the antioxidant capacity of the corresponding extract. Finally, taking into account the number of catecholic moieties as an index of the antioxidant capacity, it was hypothesized that during maturation of olive leaves: (1)

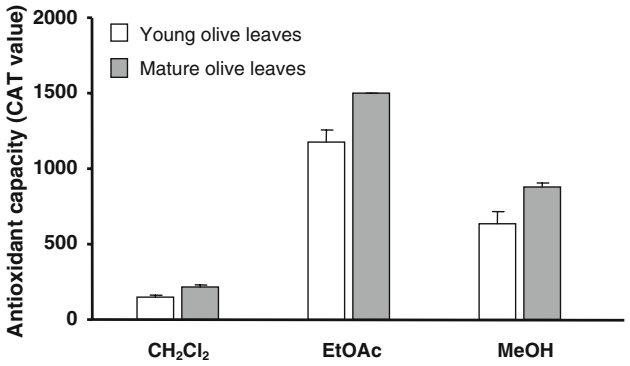

Fig. 9 CAT values (expressed in μmol Trolox/g of dried extract) of three different extracts (dichloromethane, ethyl acetate, and methanol) of young or mature olive leaves. All experiments were performed in triplicate (three wells). Results were expressed as mean ± SD

some bioconversions (oleuropein/ligstroside → verbascoside; diosmetin aglycones → glucosylated forms of luteolin) lead to an enhancement of the antioxidant capacity, (2) other bioconversions (quercetin → glucosylated forms of luteolin) lead to a decrease in antioxidant capacity, and finally (3) other bioconversions do not significantly impact the antioxidant capacity (oleuropein → oleuroside). Overall, the addition of these punctual changes (positive or negative) finally leads to a global enhancement (~25%) of the ability of mature-leaf extracts to counteract lipid oxidation in emulsions compared to young-leaf extracts. Further experiments involving CAT measurements of pure compounds have to be done to elucidate the influence of the chemical evolution of olive leaves on their antioxidant capacities.

Conclusion

In conclusion, the phenolic composition of olive leaves varies with time, likely by means of two main biochemical processes: (1) a bioconversion of flavonoids aglycones to

glucosylated flavonoids, and (2) a bioconversion of simple secoiridoids (oleuropein, oleuroside, and ligstroside) to verbascoside. This phenolic profile modification was found to impact the antioxidant capacity of the corresponding extract as evaluated by the conjugated autoxidizable triene assay. Among all extracts, the ethyl acetate extract of mature leaves exerted the highest antioxidant capacity in lipid-based multiphasic system. Finally, this result could be usefully employed in the development of new cosmetic products or food additives.

Acknowledgments Luis Javier López Giraldo thanks Programme Al*β*an, the European Union Programme of High Level Scholarships for Latin America, for the support (scholarship no. E05D055786CO). This research work was supported by the PRAD 05-14 "Lipolive" Project.

References

1. Soler-Rivas C, Espin JC, Wichers HJ (2000) Oleuropein and related compounds. J Sci Food Agric 80:1013–1023
2. Hanbury D (1854) On the febrifuge properties of the olive (*Olea europaea* L.). Pharmaceut J Provincial Trans 353–354
3. Bouaziz M, Sayadi S (2005) Isolation and evaluation of antioxidants from leaves of a Tunisian cultivar olive tree. Eur J Lipid Sci Technol 107:497–504
4. Benavente-Garcia O, Castillo J, Lorente J, Ortuño A, Del Rio JA (2000) Antioxidant activity of phenolics extracted from *Olea europaea* L leaves. Food Chem 68:457–462
5. Papoti VT, Tsimidou MZ (2009) Impact of sampling parameters on the radical scavenging potential of olive (*Olea europaea* L.) leaves. J Agric Food Chem 57:3470–3477
6. Kiritsakis K, Kontogiorgis C, Hadjipavlou-Litina D, Moustakas A, Kiritsakis A (2008) Antioxidant activity of olive leaves extracts from Greek cultivars. Planta Med 74:1188–1189
7. Salta FN, Mylona A, Chiou A, Boskou G, Andrikopoulos NK (2007) Oxidative stability of edible vegetable oils enriched in polyphenols with olive leaf extract. Food Sci Tech Int 13:413–421
8. Korukluoglu M, Sahan Y, Yigit A, Karakas R (2006) Antifungal activity of olive leaf (*Olea Europaea* L.) extracts from the Trilye region of Turkey. Ann Microbiol 56:359–362
9. Markin D, Duek L, Berdicevsky I (2003) In vitro antimicrobial activity of olive leaves. Mycoses 46:132–136
10. Lee-Huang S, Zhang L, Huang PL, Chang Y-T, Huang PL (2003) Anti-HIV activity of olive leaf extract (OLE) and modulation of host cell gene expression by HIV-1 infection and OLE treatment. Biochem Biophys Res Commun 307:1029–1037
11. Zarzuelo A, Duarte J, Jiménez J, González M, Utrilla MP (1991) Vasodilatador effect of olive leaf. Planta Med 57:417–419
12. Gonzalez M, Zarzuelo A, Gamez MJ, Utrilla MP, Jimenez J, Osuna I (1992) Hypoglycemic activity of olive leaf. Planta Med 58:513–515
13. Panizzi L, Scarpeti ML, Oriente EG (1960) Structure of the bitter glucoside oleuropein. Note II. Gazz Chim Ital 90:1449–1485
14. Heimler D, Cimato A, Alessandri S, Sani G, Pieroni A (1996) Seasonal trend of flavonoids in olive (*Olea europaea* L.) leaves. Agric Med 126:205–209
15. Fabbri A, Galaverna G, Ganino T (2008) Polyphenol composition of olive leaves with regard to cultivar, time of collection and shoot type. Acta Hort (ISHS) 791:459–464
16. Laguerre M, Lecomte J, Villeneuve P (2007) Evaluation of the ability of antioxidants to counteract lipid oxidation: existing methods, new trends and challenges. Prog Lipid Res 46:244–282
17. Laguerre M, Lopez Giraldo LJ, Lecomte J, Baréa B, Cambon E, Tchobo PF, Barouh N, Villeneuve P (2008) Conjugated autoxidizable triene (CAT) assay: a novel spectrophotometric method for determination of antioxidant capacity using triacylglycerol as ultraviolet probe. Anal Biochem 380:282–290
18. Amiot MJ, Fleuriet A, Macheix JJ (1986) Importance and evolution of phenolic compounds in olive during growth and maturation. J Agric Food Chem 34:823–826
19. De Leonardis A, Aretini A, Alfano G, Macciola V, Ranalli G (2008) Isolation of a hydroxytyrosol-rich extract from olive leaves (*Olea Europaea* L.) and evaluation of its antioxidant properties and bioactivity. Eur Food Res Technol 226:653–659
20. Kim JH, Kim BG, Park Y, Ko JH, Lim CE, Lim J, Lim Y, Ahn J-H (2006) Characterization of flavonoid 7-*O*-glucosyltransferase from *Arabidopsis thaliana*. Biosci Biotechnol Biochem 70:1471–1477
21. Wright JS, Johnson ER, DiLabio GA (2001) Predicting the activity of phenolic antioxidants: theoretical method, analysis of substituent effects, and application to major families of antioxidants. J Am Chem Soc 123:1173–1183
22. Bors W, Heller W, Michel C, Saran M (1990) Flavonoids as antioxidants: determination of radical-scavenging efficiencies. Methods Enzymol 186:343–355